Colloids and Surfaces B: Biointerfaces 220 (2022) 112962

Contents lists available at ScienceDirect

Colloids and Surfaces B: Biointerfaces

journal homepage: www.elsevier.com/locate/colsurfb

Correlation between biological responses *in vitro* and *in vivo* to Ca-doped sol-gel coatings assessed using proteomic analysis

I. García-Arnáez [a,*,1], F. Romero-Gavilán [b,1], A. Cerqueira [b], F. Elortza [c], M. Azkargorta [c], F. Muñoz [d,e], M. Mata [f,g], J.J. Martín de Llano [f,g], J. Suay [b], M. Gurruchaga [a], I. Goñi [a]

[a] Department of Polymers and Advanced Materials: Physics, Chemistry and Technology, University of the Basque Country (UPV/EHU), P. M. de Lardizábal, 3, 20018 San Sebastián, Spain
[b] Department of Industrial Systems Engineering and Design, Universitat Jaume I, Av. Vicent Sos Baynat s/n, 12071 Castellón de la Plana, Spain
[c] Proteomics Platform, CIC bioGUNE, Basque Research and Technology Alliance (BRTA), CIBERehd, ProteoRed-ISCIII, Bizkaia Science and Technology Park, 48160 Derio, Spain
[d] Department of Veterinary Clinical Sciences. Facultade de Veterinaria, Universidade de Santiago de Compostela, Campus Universitario, s/n, 27002 Lugo, Spain
[e] iBoneLab SL, Avenida da Coruña 500, 27003 Lugo, Spain
[f] Department of Pathology Medicine and Odontology, Medicine Faculty, University of Valencia, Av Blasco Ibáñez, 13, 46010 Valencia, Spain
[g] Research Institute of the University Clinical Hospital of Valencia (INCLIVA), C. de Menéndez y Pelayo, 4, 46010 Valencia, Spain

ARTICLE INFO

Keywords:
Implants
In vitro in vivo correlation
Proteomics
Coagulation
Inflammation
Bone regeneration

ABSTRACT

Poor correlation between the results of *in vitro* testing and the subsequent *in vivo* experiments hinders the design of biomaterials. Thus, new characterisation methods are needed. This study used proteomic and histological techniques to analyse the effects of Ca-doped biomaterials *in vitro* and *in vivo* and verify the correlation between the two systems. The sol-gel route was employed to synthesise coatings functionalised with 0.5 and 5 wt% of $CaCl_2$. Morphology of the coatings was examined using SEM; the Ca^{2+} ion release from the materials was analysed by means of ICP-AES spectroscopy. The osteogenic and inflammatory responses were inspected *in vitro* in human osteoblasts (HOb) and TPH-1 monocytes. The *in vivo* experiments used a rabbit model. The nLC-MS/MS-based proteomic methods were utilised to analyse the proteins adhering to the material samples incubated with human serum or examine protein expression in the tissues close to the implants. Ca-doped biomaterials caused a remarkable increase in the adsorption of coagulation-related proteins, both *in vitro* (PLMN, THRB, FIBA and VTNC) and *in vivo* (FBLN1, G1U978). Enhanced affinity to these materials was also observed for proteins involved in inflammation (CO5, C4BPA, IGHM and KV302 *in vitro*; CARD6, DDOST and CD14 *in vivo*) and osteogenic functions (TETN, PEDF *in vitro*; FBN1, AHSG, MYOC *in vivo*). The results obtained using different techniques were well matched, with a good correlation between the *in vitro* and *in vivo* experiments. Thus, the proteomic analysis of biological responses to biomaterials *in vitro* is a useful tool for predicting their impact *in vivo*.

1. Introduction

The development of new biomaterials is a complex process. The biological evaluation of these materials is conducted using *in vitro* and *in vivo* tests and clinical studies. Unfortunately, a material with excellent *in vitro* properties can precipitate a disastrous *in vivo* outcome; the data obtained from these two experimental systems are often poorly correlated [1]. This can result in considerable economic losses and a waste of resources. Thus, new methods for characterising biomaterials [2] are needed to predict their effects reliably after implantation [3].

Using *in vitro* and *in vivo* proteomic methods could overcome the limitations of traditional testing. The response to biomaterials is strongly affected by the initial adsorption of proteins. Improved understanding of the interactions between these proteins and the material would allow predicting the biological responses to implantation and help in biomaterial design [4,5].

* Correspondence to: Departamento de Polímeros y Materiales Avanzados: Física, Química y Tecnología, Laboratorio de Biomateriales Poliméricos, Campus de Gipuzkoa, Paseo Manuel de Lardizabal 3, 20018 Donostia, Spain.
E-mail address: inaki.garciaa@ehu.eus (I. García-Arnáez).
[1] co-autorship.

https://doi.org/10.1016/j.colsurfb.2022.112962
Received 15 July 2022; Received in revised form 10 October 2022; Accepted 20 October 2022
Available online 21 October 2022

Calcium is an element commonly used in the development of biomaterials due to its involvement in bone metabolism and coagulation. The Ca^{2+} ions condition the tissue–material interface, affecting protein deposition on the biomaterial and the cellular responses [6].

The Ca^{2+} ions promote and accelerate blood coagulation. The blood clot around the implant serves as an initial scaffold for tissue repair, bone mineralisation and subsequent remodelling [7,8]. These ions act at various stages of the intrinsic and extrinsic pathways of the coagulation cascade, leading to the formation of the prothrombinase complex. The complex converts prothrombin into thrombin, crucial for stimulating osteoblast differentiation and increasing osteogenesis [9]. Gessmann et al. state that calcium plays an important role in the formation of clots, which affects tissue regeneration [10]. Thus, the chemical modification of dental implant surfaces with calcium ions results in a strong pro-coagulant effect, providing instant stability. The proteomic analysis of protein adsorption on a Ca-biomimetic surface, carried out by our group, has shown a remarkably increased affinity of factor X protein, involved in the common pathway of the coagulation cascade [11]. In another study of protein adsorption and desorption dynamics on Ca-enriched titanium surfaces, we have observed that the calcium-doping enhances the affinity for proteins related to coagulation (FA10, THRB, ANT3), suggesting an increase in the coagulatory potential of these materials [12]. We have also found that the incorporation of $CaCl_2$ into a 3-(glycidoxypropyl)-trimethoxysilane-based sol-gel coating increases the adsorption of serum proteins associated with the coagulation pathway (such as THRB, ANT3, PROS, PROC, A2AP and A2MG)[6]. This preferential adsorption of coagulation-related proteins on surfaces doped with calcium ions could promote the pro-coagulation cascade response. Thus, the fibrin production would be accelerated and implant stability expedited [11,13].

The complement system is activated during blood coagulation, increasing the thrombogenic properties of blood through the inhibition of anticoagulation mechanisms. Multiple regulatory loops linking the two systems are activated simultaneously to synchronise effective responses [14]. In our previous reports, we have observed that the addition of calcium affects inflammatory processes in a dose-dependent manner [6]. The expression of an immune-response gene TNF-α is augmented by the Ca-supplemented materials. The increased adhesion of C1QC protein might be related to the enhanced inflammatory response observed in the *in vitro* experiments. Furthermore, the adsorption of three proteins involved in immune response (LYSC, PIP and SAMP) significantly increases on the Ca-doped surfaces [11]. Besides, the initial inflammation is associated with increased adsorption of complement proteins to these materials. However, as this pro-inflammatory effect disappears once the calcium is released, the Ca-containing surfaces should not cause a chronic inflammatory reaction [12].

The aim of this study was to improve bone regeneration, improving coagulation. Furthermore, we used proteomic techniques to analyse the effects of Ca-doped biomaterials in the *in vitro* and *in vivo* experimental systems and to examine the level of correlation between the results obtained for the two systems. To achieve that, a sol-gel coating, previously designed by our group [15], was doped with increasing amounts of Ca (0 %, 0.5 % and 5 %). The network contained 70 % of MTMOS and 30 % of TEOS (molar percentages) because it showed good osteointegration and osteogenic activity both *in vitro* and *in vivo* [16]. The behaviour of these new Ca-enriched materials was examined in cell cultures and *in vivo* experiments. The *in vitro* adsorption of serum proteins onto the biomaterial surfaces and the protein profiles of tissues surrounding the implant (*in vivo*) were analysed using MS-based proteomics. The cellular responses *in vitro*, the *in vivo* histological analysis and proteomic evaluations for both systems showed correlations between the results for the inflammatory, coagulation and bone regeneration processes.

2. Materials and methods

2.1. Material synthesis and sample preparation

The silica precursors selected to obtain the sol-gel coatings were methyltrimethoxysilane (MTMOS [M]; Merck, St. Louis, MO, USA) and tetraethyl orthosilicate (TEOS [T]; Merck) in a molar ratio of 7:3, respectively, following the methods described in the previous studies [15]. The solvent used in the synthesis was 2-propanol (50 % v/v). The hydrolysis was conducted by adding the stoichiometric amount of acidified water with HNO_3 (0.1 M). The resulting material was functionalised with 0.5 and 5 wt% of $CaCl_2$, as reported in Romero-Gavilán et al. [6]. The sol-gel mixtures were kept for 1 h under stirring and then 1 h at rest. Grade-4 commercially pure Ti discs (10-mm and 12-mm diameter and 1.2-mm thickness; GMI Dental Implantology SL, Lleida, Spain) and custom-made implants (3-mm diameter at the top and 2-mm diameter at the bottom, 4-mm long; GMI Dental Implantology SL) were sandblasted, acid-etched and then coated with prepared materials by dip-coating, following the procedures described previously [16]. To obtain the samples for the Ca^{2+} release studies, glass slides were coated by casting.

2.2. Morphological characterisation and Ca^{2+} release

The morphology of the surfaces was characterised by scanning electron microscopy (SEM), using the Leica-Zeiss LEO 440 microscope (Leica, Wetzlar, Germany). The materials were submitted to platinum sputtering to increase their conductivity for the SEM observations. The amount of released Ca^{2+} was evaluated (in triplicate) using inductively coupled plasma atomic emission spectroscopy (ICP-AES) (Activa, Horiba Jobin Yvon IBH Ltd., Glasgow, UK). The wavelengths are 396.847 nm (to quantify) and 317.933 nm (to confirm). LOQ is 0.01 mg/L and Perade-09 is used as Certified Reference Material. The coatings were immersed in 50 mL of ultrapure water at 37 °C. After 2, 4, 8, 24, 72, 168, 336, 504 and 672 h of immersion, a 0.5-mL sample was removed, and the Ca^{2+} concentration was determined.

2.3. In vitro assays

2.3.1. Cell culture

Human osteoblasts (HOb) derived from healthy bone (Cell Applications Inc., San Diego, CA, USA) were suspended in a proliferation medium consisting of low-glucose Dulbecco's Modified Eagle's Medium enriched with 4 mM L-glutamine (DMEM; Merck), with 1 % penicillin/streptomycin (Gibco, Thermo Fisher Scientific, Waltham, MA, USA) and 10 % foetal bovine serum (FBS; Gibco). After 24 h, the cells were seeded on the coated discs at 2.5×10^4 cells/cm^2 in an osteogenic medium of DMEM, 1 % penicillin/streptomycin, 10 % FBS, 1 % ascorbic acid (5 μg/mL) and 100 mM β-glycerol phosphate. The cells were cultured for 7 and 14 days at 37 °C in a humidified (95 %), 5 %-CO_2 atmosphere. The cell culture medium was changed every 48 h.

TPH-1 cell line was seeded on the materials at of 30×10^4 cells/cm^2 for 1 day and 15×10^4 cells/cm^2 for 3 days in RPMI-1640, supplemented with 1 % penicillin/streptomycin and 10 % FBS, in a cell incubator (90 % humidity, 37 °C, 5 % CO_2). Their differentiation into macrophages was induced by phorbol 12-myristate 13-acetate.

2.3.2. Proliferation

For measuring HOb cell proliferation, the alamarBlue™ cell viability assay (Invitrogen-Thermo Fisher Scientific, Waltham, MA, USA) was used following the manufacturer's protocol. The assay is based on the redox reaction with resazurin. The cells were cultured with the discs (three replicates per material) and examined after 1, 3 and 7 days. The results (percentage of reduced resazurin) were used to assess cell proliferation.

2.3.3. Quantitative real-time PCR

Quantitative real-time PCR (qRT-PCR) was employed to examine the effect of the Ca-doped materials on gene expression. Total RNA was isolated using the TRIzol method described by Cerqueira et al. [17]. Table S1 shows the targets studied. A total of 6 replicates were done for PCR experiments. The data was normalized following the $2^{-\Delta\Delta Ct}$ method. PCR reactions were carried out under the conditions described in Cerqueira et al. [18].

2.3.4. Cytokine quantification using ELISA

The levels of tumour necrosis factor-alpha (TNF-α) and transforming growth factor-beta (TGF-β) were measured in the culture medium of TPH-1 cells incubated on the discs for 1 and 3 days. The concentration was determined using an ELISA assay kit (Thermo Fisher Scientific) following the manufacturer's instructions.

2.4. Proteomic evaluation

2.4.1. In vitro experiment

Each titanium disk was incubated in a well of a 24-well NUNC plate (Thermo Fisher Scientific, Waltham, MA, USA) with 1 mL of human serum obtained from male AB plasma (Merck) for 180 min at 37 °C and 5 % CO_2.

Then, the serum was removed, and the samples were subjected to 5 consecutive washes with 200 μL of milli-Q water. To remove non-adsorbed proteins, the discs were rinsed with 200 μL of a 100 mM NaCl solution in 50 mM Tris-HCl at pH 7. The adsorbed proteins were eluted with a solution of 4 % sodium dodecyl sulphate (SDS), 100 mM dithiothreitol (DTT) and 0.5 M triethylammonium bicarbonate buffer (TEAB; Merck).

Four independent replicates were processed for each surface type; each replicate was prepared by pooling the eluates from 4 discs.

2.4.2. In vivo experiment

The *in vivo* experiment was performed using 16 adult (26–28 weeks old, mean weight of 4.5 kg) healthy New Zealand White male rabbits (Granja San Bernardo, Navarra, Spain). The animals were hosted in individual cages in a research facility (Animalario experimental del campus de Lugo) after obtaining the ethical agreement (Code of procedure: 06/18/LU-002) and under strict conditions of humidity, temperature and light cycles. The rabbits were fed sterile pellets, had free access to water and were monitored daily throughout the experiment.

The animals were randomly allocated to each treatment group using closed envelopes that were opened just before the procedures. On the day of the surgery, each rabbit was assigned a number, which was marked on the inner sides of both ears. Each cage was identified with the same number; it accompanied the animal during the cage changes.

Bone implantation sites were selected following the guidelines in International Standard ISO 10993 "Biological Evaluation of Medical Devices" Part 6:2016 in Annex C, "Tests for bone tissue effect after implantation". Seven implants of each material type were used in a rabbit femoral condyle model. The different materials to be tested were randomly assigned to the left or right side, according to a computer-generated randomisation list, until the same number in each of the positions (anterior and posterior, right and left) was reached.

All surgical procedures were performed in an operating room after a quarantine period under sterile conditions. The animals were first premedicated with a combination of medetomidine (Sededorm, 50 μg/kg/i.m.; Vetpharma Animal Health SL, Barcelona, Spain), ketamine (Ketamidor, 25 mg/kg/i.m.; Richter Pharma AG, Wels, Austria) and a single dose of enrofloxacin (Syvaquinol, 5 mg/kg/s.c.; Laboratorios Syva, León, Spain). The general inhalational anaesthesia was induced and maintained using 2.5–4 % isoflurane (Vetflurane, Virbac SA, Carros, France). Once the surgery was finished, atipamezole (Nosedorm, 150 μg/kg/i.m.; Vetpharma Animal Health SL) was administered to reverse the effects of medetomidine.

After aseptic preparation of the skin, a lateral approach to the lateral femur was performed, sectioning the skin and subcutaneous tissue, dissecting the musculature and exposing the surface of the lateral condyle with a periosteal elevator. Two implants per femur were placed using a surgical motor (INTRAsurg 300, KaVo Dental Excellence, Biberach an der Riss, Germany). The muscle, subcutaneous tissue and skin were closed with continuous absorbable sutures (Vicryl 4–0, Ethicon, Raritan, NJ, USA).

Each animal received the peri- and post-operative analgesia using buprenorphine (Bupaq, 0.3 mg/kg/i.m.; Richter Pharma AG) and enrofloxacin in drinking water (1 mL/L, Syvaquinol) as antibiotic prophylaxis (for 21 days). Meloxicam was used as pain control for three days (Loxicom, first day, 0.2 mg/kg/s.c., the next two days, 0.1 mg/kg orally; Norbrook Laboratories Limited, Monaghan, Ireland).

Rabbits were euthanised 5 days after implantation by an intravenous overdose of sodium pentobarbital (100 mg/kg IV, Dolethal, Vétoquinol Especialidades Veterinarias SA, Madrid, Spain) after sedation with a combination of medetomidine (Sededorm, 50 μg/kg/i.m.; Vetpharma Animal Health SL) and ketamine (Ketamidor, 25 mg/kg/i.m.; Richter Pharma AG).

The distal femurs were dissected to examine the macroscopic appearance of the implanted materials. For proteomics, the implants were recovered individually using a trephine with a 3.9-mm internal diameter, 5-mm external diameter and a biopsy length of 8 mm (Komet). Subsequently, the specimens were placed in 0.5-mL tared Eppendorf tubes (weighed empty), and the tubes were weighed again and kept frozen at −80 °C. The implants and surrounding bone for histology examination were immersed in a 10 % buffered formalin solution.

The frozen tissue was mechanically broken to separate the bone from implants. Bone pieces were incubated with cell lysis buffer (7 M urea, 2 M thiourea, 4 % CHAPS and 10 mM DTT) and homogenised in a Precellys homogeniser (Bertin Instruments, Montigny-le-Bretonneux, France). Extracted proteins were digested following the filter-aided sample preparation (FASP) protocol described by Wiśniewski et al. [19], with minor modifications. Trypsin was added to trypsin:protein ratio of 1:20, and the mixture was incubated for 2 h at 37 °C. After recovery, the peptides were dried in an RVC2 25 speedvac concentrator (Christ, Osterode am Harz, Germany) and resuspended in 0.1 % formic acid (FA). The peptides were desalted and resuspended in 0.1 % FA using C18 stage tips (Agilent, Santa Clara, CA, USA).

2.4.3. Protein identification and bioinformatic data analysis

For proteomic analysis of *in vitro* samples, the protocol described by Romero-Gavilan et al. [1] was followed. Liquid chromatography-tandem mass spectrometry (LC-MS/MS) approach was used, employing a nanoACQUITY UPLC system (Waters, Milford, MA, USA) coupled with an Orbitrap XL spectrometer (Thermo Electron, Bremen, Germany). Progenesis QI software (Nonlinear Dynamics, Newcastle, UK) was used for the differential analysis of the proteins identified on the studied surfaces.

In vivo samples were analysed in a hybrid trapped ion-mobility–quadrupole time-of-flight mass spectrometer (timsTOF Pro with PASEF, Bruker Daltonics, Bremen, Germany) coupled online to an EvoSep ONE liquid chromatograph (EvoSep, Odense C, Denmark). The digested bone proteins (200 ng) were directly loaded onto an EvoSep ONE chromatograph and the profiles were acquired using the 30 SPD protocol.

Protein identification and quantification were carried out using the MaxQuant software [20] with default settings (except for the LFQ minimum ratio count of 1). The searches were performed against the UniProt/Swiss-Prot database of human proteins with precursor and fragment tolerances of 20 mg/L and 0.05 Da, respectively. Only the proteins with at least two peptides at FDR < 1 % were considered for further analysis. The data (LFQ intensities) were loaded onto the Perseus platform [21] and further processed (log2 transformation, imputation). The detected proteins were classified by function using PANTHER

(Protein ANalysis THrough Evolutionary Relationships, www.pantherdb.org), DAVID (the Database for Annotation, Visualization and Integrated Discovery, david.ncifcrf.gov) and UniProt tools [22].

2.5. Histological preparation

The blocks containing the lateral femoral condyle were prepared following the guidelines described by Donath & Breuner [23]. Briefly, the femoral condyles were dehydrated using graded ethanol series (70–100 %) and infiltrated with different graded mixtures of ethanol and glycol methacrylate (Technovit 7200 VLC, Heraeus Kulzer, Wehrheim, Germany). The samples were then polymerised and processed to obtain a central section of the implant of approximately 200 μm. This section was micro-ground employing the Exakt grinding system (Exakt Apparatebau, Norderstedt, Germany) using 1200 to 4000 Grit silicon carbide papers (Struers, Copenhagen, Denmark). Sections of approximately 40 μm were stained using the Levai–Laczkó method [24].

Digital images of tissues surrounding the implant threads were recorded with a bright-field Leica DM4000 B microscope and a DFC420 digital camera using 1.6× and 20× objectives.

2.6. Statistical analysis

Cell culture results were subjected to a one-way analysis of variance (ANOVA) and the Newman-Keuls multiple comparison post-hoc test. Differences between control (MT) and the Ca-doped coatings were considered statistically significant at $p \leq 0.05$ (*), $p \leq 0.01$ (**) and $p \leq 0.001$ (***). In proteomic evaluations, the Student's *t*-test was applied to identify statistically significant differences. Proteins were considered differentially adsorbed when their abundance ratio (for two different conditions) was larger than 1.5 in either direction, and the differences were statistically significant ($p \leq 0.05$).

3. Results

3.1. Morphological characterisation and Ca^{2+} release

The Ca-doped sol-gel compositions were successfully synthesised and applied as coatings on titanium, resulting in homogeneous coatings without cracks or pores, as seen in the SEM microphotographs (Fig. 1A–C).

Fig. 1D shows the kinetic liberation of Ca^{2+} from coatings with 0.5 % and 5 % of Ca. Increasing the $CaCl_2$ content in the network boosts the Ca release. The fastest Ca release happens during the first two hours.

3.2. Cell culture experiments

3.2.1. Effects on macrophages (inflammatory responses)

The liberation of TNF-α, a marker of inflammation, increased significantly after 1 and 3 days of culture with the material containing 5 % Ca compared to MT. The level of this protein seems to be dependent on calcium content, indicating that Ca might enhance the pro-inflammatory effect (Fig. 2A). The same trend is also observed for the expression of the IL-1b gene, which increases in a Ca dose-dependent manner, suggesting an increase in the inflammatory potential with growing calcium content (Fig. 2B).

In contrast, the secretion of the TGF-β, an anti-inflammatory marker, does not change in the cells grown on any of the tested coatings (Fig. 2C). The IL-10 gene expression (one of the main anti-inflammatory markers) only increases after 3 days of culture for the material doped

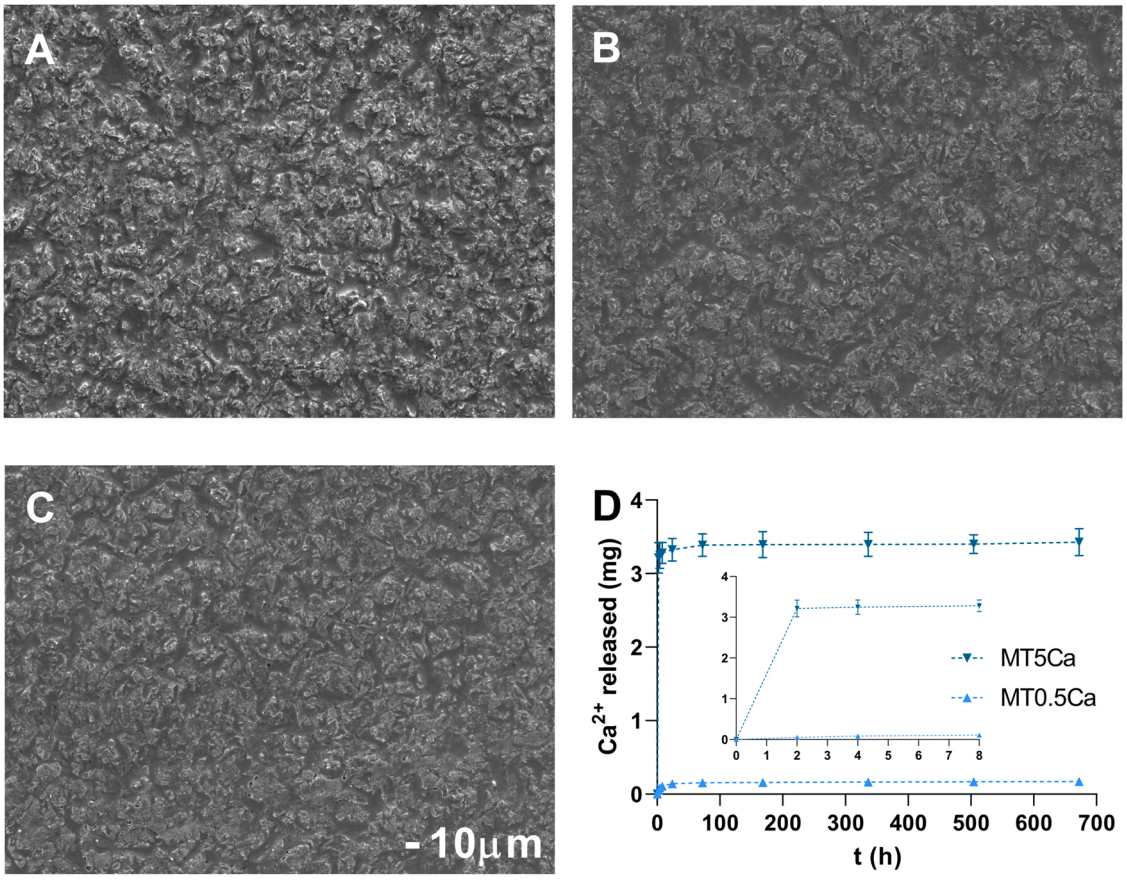

Fig. 1. SEM microphotographs of MT (A), MT0.5Ca (B) and MT5Ca (C); × 300. Scale bars, 10 μm. Ca^{2+} release from the sol-gel coatings (D). 3 replicates were applied. Results are shown as means ± SD.

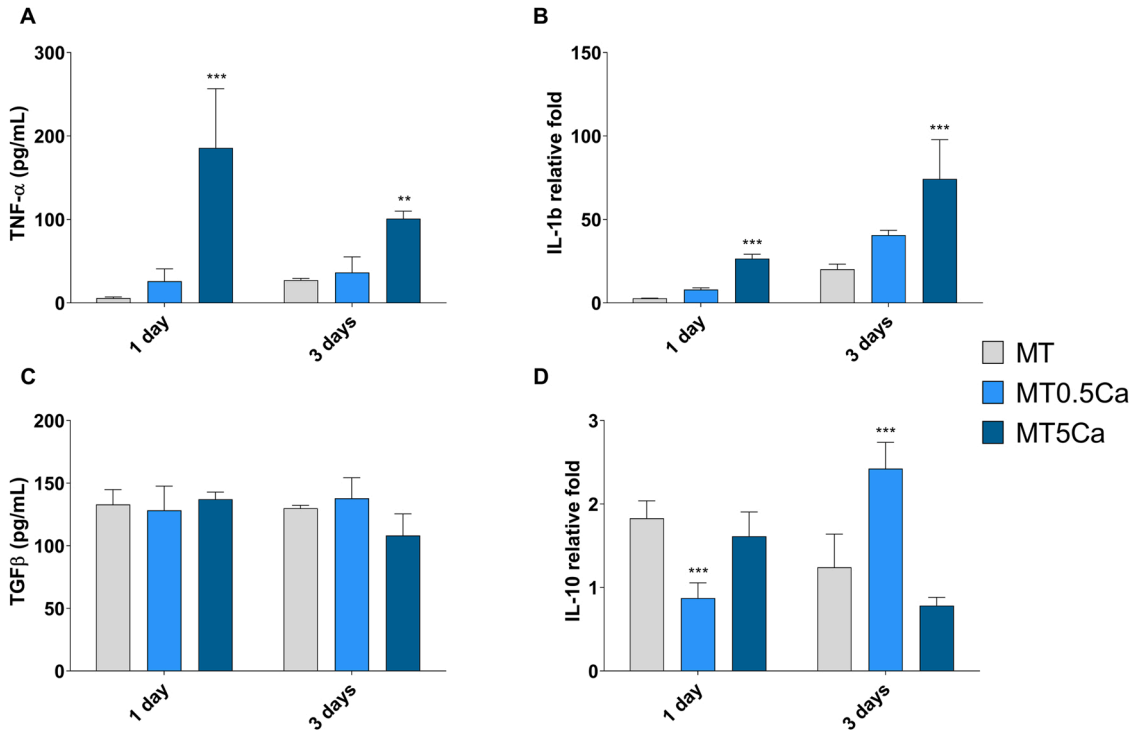

Fig. 2. Evaluation of inflammatory markers: TNF-α cytokine (A) and TGF-β cytokine (C) release measurement using ELISA; and relative gene expression of IL-1b (B) and IL-10 (D) measured by qRT-PCR in the THP1 cells cultured on the different Ca-containing coatings for 24 and 72 h. A total of 3 replicates for ELISA measurements and 6 replicates for PCR were applied. The results are shown as means ± SD. The asterisks ($p \leq 0.01$ (**) and $p \leq 0.001$ (***)) indicate the statistical significance of differences between the MT and Ca-doped MT.

with 0.5 % Ca; its expression on this material is the lowest of all after the first 24 h (Fig. 2D).

3.2.2. *Effects on osteoblasts (osteogenic responses)*

In the human osteoblasts (HOb) cultured with the sol-gel materials, gene expression of osteogenic markers RUNX2 and OCN did not vary significantly. For COL1, it tended to decrease for all Ca concentrations

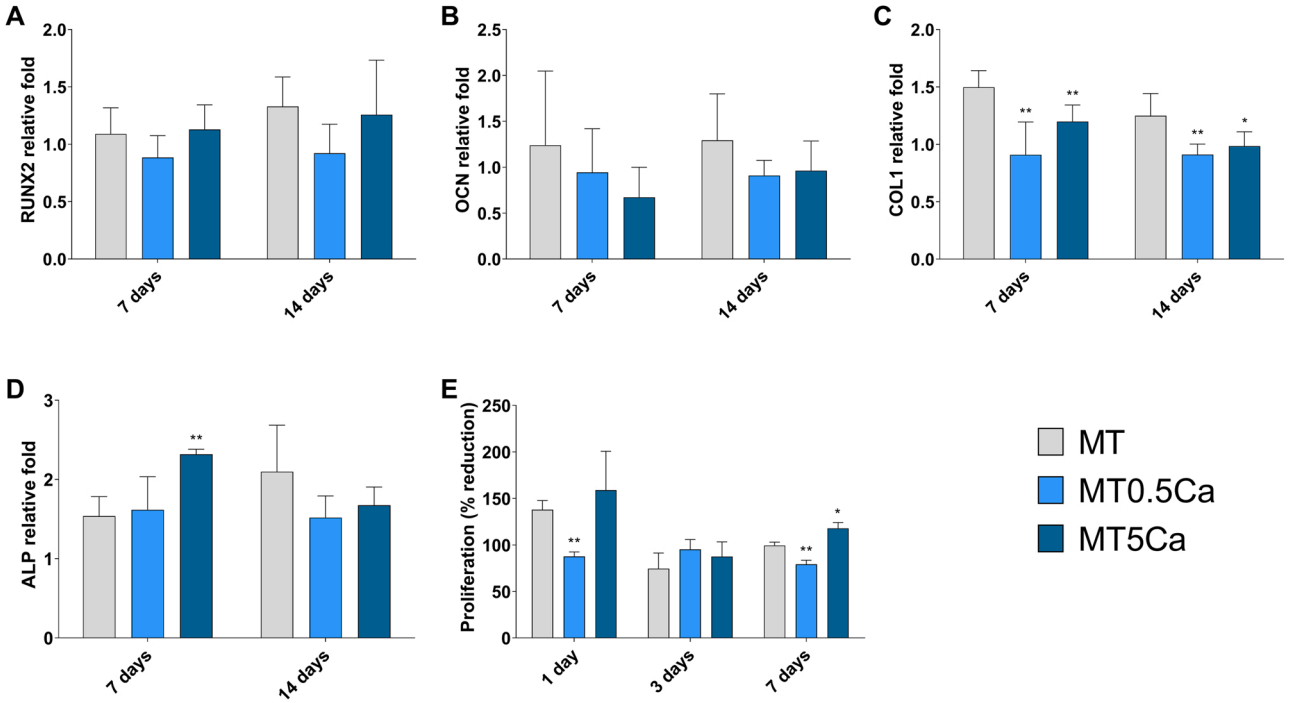

Fig. 3. Relative gene expression levels of the osteogenic markers RUNX2 (A), OCN (B), COL1 (C) and ALP (D) in the HOb cells cultured on different Ca-containing coatings for 7 and 14 days. (E) HOb cell proliferation after 1, 3 and 7 days. A total of 3 replicates for proliferation measurements and 6 replicates for PCR were applied. Results are shown as means ± SD. The asterisks ($p \leq 0.05$ (*), $p \leq 0.01$ (**)) indicate the statistical significance of differences between MT and Ca-doped MT.

(0.5 % and 5 %) in comparison with MT (Fig. 3). In contrast, an increase in ALP expression was observed on MT5Ca coating after 7 days. Furthermore, the analysis of cell proliferation showed a peak in cell growth after 7 days of incubation with MT5Ca.

3.3. Proteomic analysis

3.3.1. In vitro experiment

The eluates of proteins adsorbed to the sol-gel coatings were analysed using the LC-MS/MS technique, identifying 107 different proteins. The Progenesis QI software was employed for statistical comparisons of relative quantities of the proteins adhering to the Ca-coatings and those bound to the reference sol-gel material (MT). The DAVID and PANTHER databases and UniProt tools were used to classify these proteins according to their functions.

The results of the comparative analysis (Progenesis QI) are shown in Table 1. Nineteen proteins increased their adsorption levels on Ca-doped sol-gels compared to the reference samples.

Some of the 19 proteins with increased affinity for Ca-containing materials have functional links to the immune and complement system. The analysis revealed proteins associated with the activation of the complement system (CO5) and its inhibition (CLUS, C4BPA, CFAH, IC1 and VTNC) and the immunoglobulins IGHM and KV302. Some other proteins preferentially binding to Ca-doped materials were related to the processes of blood coagulation and fibrinolysis (HRG, FIBA, THRB, PROS, PLF4 and PLMN). Similarly, we observed increased adsorption of proteins (such as PEDF) linked to the development of new bone. Enhanced binding of TETN, involved in implant integration processes such as the cell adhesion, extracellular matrix and bone mineralisation, was also detected.

Fig. 4 illustrates the Ca dose-dependent changes in the normalised abundance of proteins linked to the processes triggered by implantation. Thus, the proteins related to inflammation (blue), coagulation (red), fibrinolysis (black) and bone regeneration (green) are shown.

Table 1
The Progenesis analysis of proteins differentially adsorbed onto Ca-enriched coatings in comparison with the base material. The detected proteins with ANOVA $p < 0.05$ (yellow) and a ratio higher than 1.5 (green) were considered significantly different (bold). Proteins are shown using their UniProt ID (without the "_HUMAN" suffix).

		MT0.5Ca vs MT		MT5Ca vs MT	
Code	**Protein**	***p***	**Ratio**	***p***	**Ratio**
HRG	Histidine-rich glycoprotein	**0.004**	**2.41**	**0.000**	**6.82**
PLF4 PF4V	Platelet factor 4	**0.046**	**4.82**	0.054	6.70
APOC4	Apolipoprotein C-IV	**0.015**	**3.58**	**0.001**	**5.10**
PLMN	Plasminogen	**0.018**	**1.76**	**0.033**	**3.30**
C4BPA	C4b-binding protein alpha chain	**0.004**	**2.68**	**0.001**	**3.29**
PROS	Vitamin K-dependent protein S	0.080	1.58	**0.001**	**3.21**
CD5L	CD5 antigen-like	0.554	1.24	**0.013**	**3.14**
CLUS	Clusterin	0.060	1.96	**0.017**	**2.99**
FIBA	Fibrinogen alpha chain	0.425	1.36	**0.037**	**2.75**
IGHM	Ig mu chain C region	**0.021**	**1.69**	0.067	2.56
IC1	Plasma protease C1 inhibitor	**0.004**	**1.65**	0.056	2.52
VTNC	Vitronectin	**0.043**	**1.40**	0.084	2.10
APOC3	Apolipoprotein C-III	0.057	1.68	**0.035**	**2.03**
CO5	Complement C5	**0.047**	**1.64**	0.139	2.00
KV302	Ig kappa chain V-III region SIE	**0.003**	**1.78**	0.056	1.97
THRB	Prothrombin	0.393	1.40	**0.049**	**1.72**
PEDF	Pigment epithelium-derived factor	**0.024**	**1.71**	0.060	1.59
CFAH	Complement factor H	**0.039**	**1.71**	0.128	1.44
TETN	Tetranectin	**0.037**	**1.48**	0.429	1.24

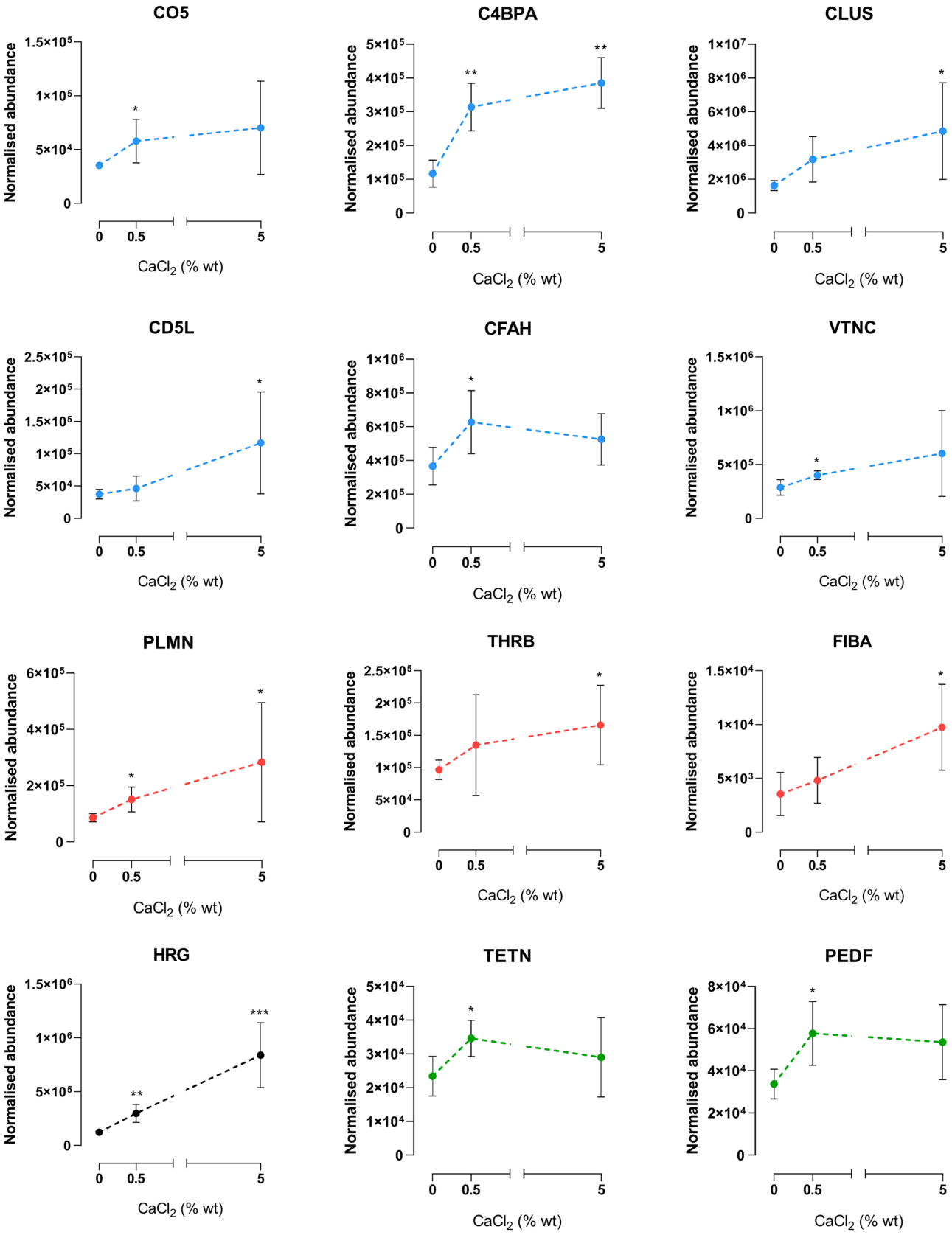

Fig. 4. The normalised abundance of 12 differentially adsorbed proteins with key functions in regeneration: inflammation (blue), coagulation (red), fibrinolysis (black) and bone regeneration (green). Results are shown as means ± SD. The asterisks ($p \leq 0.05$ (*), $p \leq 0.01$ (**) and $p \leq 0.001$ (***)) indicate the statistical significance of differences between MT and Ca-doped MT.

The PANTHER programme classifies proteins according to their links to the signalling pathways and their biological processes. Fig. 5 shows that coagulation is the main pathway associated with the proteins differentially adsorbed to the materials doped with $CaCl_2$ (especially to MT5Ca). Associations with other pathways were also detected, in varying proportions, depending on the percentage of Ca incorporated into the coating. Thus, the activation of B cells, related to the complement system [25], appeared for the coatings with 0.5 % Ca. CCKR signalling, with an effect on angiogenesis [26], was associated with proteins found on materials with 5 % Ca. Functions related to the activation of the plasminogen cascade, which affects fibrinolysis [27] were also identified for the proteins with increased affinity to Ca-surfaces. Among the various biological functions detected, the immune system, cellular process, metabolic process, response to stimulus, biological adhesion and localisation were associated with the proteins differentially adsorbed on Ca-materials. For MT0.5Ca, the proteins linked to biogenesis, multicellular organismal process and biological regulation functions also appeared.

3.3.2. *In vivo experiment*

The proteomic profiles of tissues surrounding the non-doped and Ca-doped coated implants were analysed by nLC-MS/MS, identifying 2258 different proteins. The Progenesis QI analysis revealed that the levels of 76 of these proteins were different in tissues in contact with MT0.5Ca and MT5Ca implants in comparison with MT (Table S2). Of these, 33 were found in smaller amounts in the tissue surrounding the Ca-doped implant surfaces than in the reference sample (MT). The levels of the remaining 43 proteins tended to increase in the tissues in contact with Ca-enriched coatings.

Fig. 6 shows the Ca content-dependent changes in the normalised abundance of the main proteins related to inflammation processes (CARD6, CD14, SERPING1 and DDOST; blue), coagulation (FBLN1 and G1U978; red) and bone regeneration (FBN1, AHSG and MYOC; green).

3.4. *In vivo experiments. Histology*

As shown in Fig. 7A–C, there were some bone particles and debris in the medullary bone cavity, close to the titanium implants. These particles of damaged bone tissue contained empty osteocyte lacunae. The implant grooves were lined with the sol-gel coating. There was a tenuous, faint matrix filling the space of the grooves and near the crests of the implants. These were probably the remnants of the fibrin-rich matrix from the initial peri-implant blood clot formed after surgery. Some sparse erythrocyte clumps from the initial blood clot were observed in this matrix in the MT and MT0.5Ca implants (Fig. 7A1 and B1, respectively). The erythrocyte clumps were larger and found more often on the MT5Ca than on other implant types (Fig. 7C1). Another difference between the implants was the number of mesenchymal cells with a fibroblastic morphology found near the implant surface. Few fibroblast-like cells were observed in the proximity of the MT implant (Fig. 7A2), while they were abundant in the apical portion of MT0.5Ca and MT5Ca calcium-doped implants (Fig. 7B2 and C2).

4. Discussion

The biological evaluation of biomaterials is achieved by performing *in vitro*, *in vivo* and clinical studies. The *in vitro* studies should predict the biological response; the osteoblast maturation leading to bone formation

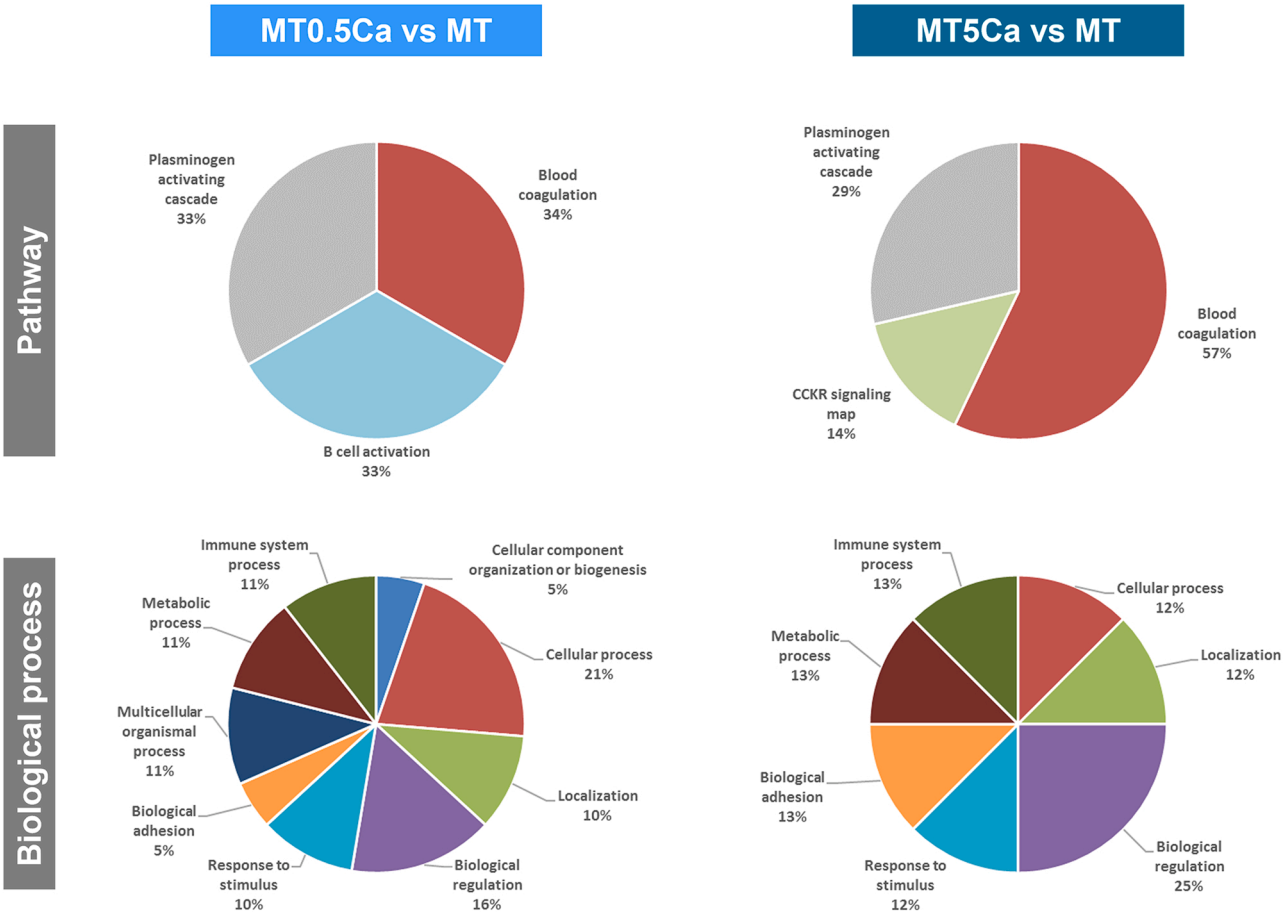

Fig. 5. PANTHER diagram with the pathway functions and biological processes linked to the proteins with increased adherence to Ca-enriched sol-gel coatings in comparison with the reference sample (MT).

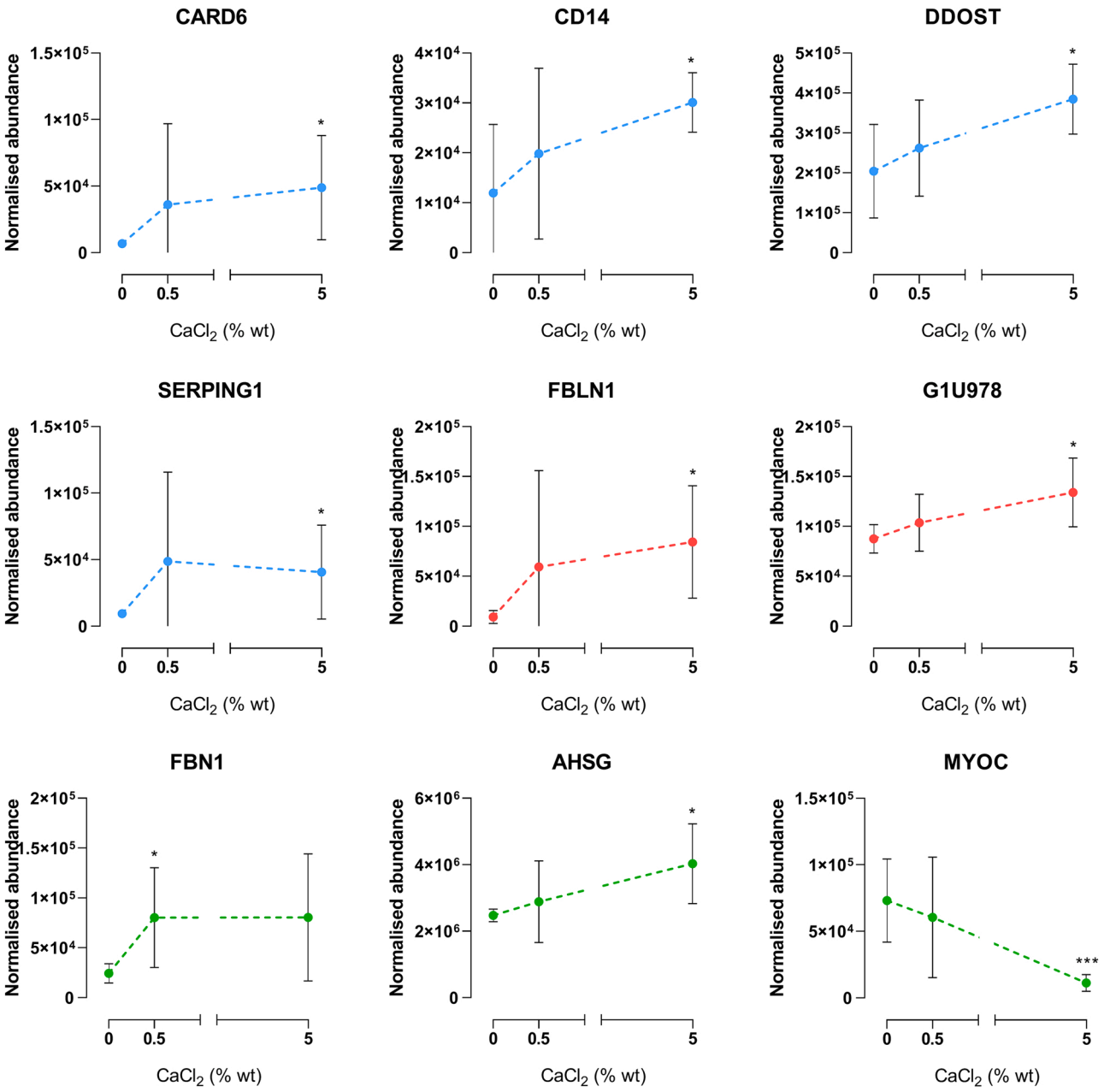

Fig. 6. The normalised abundance of 9 proteins differentially expressed *in vivo*, with key functions in regeneration: inflammation (blue), coagulation (red) and bone regeneration (green). Results are shown as means ± SD. The asterisks ($p \leq 0.05$ (*), $p \leq 0.01$ (**) and $p \leq 0.001$ (***)) indicate the statistical significance of differences between MT and Ca-doped MT.

has received much attention. This process, among others, can be tested in an *in vivo* model, and the response to biomaterials should be observed in real-life situations. Unfortunately, there is a surprisingly poor correlation between the results obtained *in vitro* and *in vivo* [2]. This unexpectedly low correlation could be due to the fact that cell cultures are relatively simple systems compared to the complexity of living tissues. Moreover, the principal focus of the studies in this field has been osteoblast maturation, and other key aspects like the immune and coagulation systems have been neglected.

Despite the weaknesses of the widely used traditional *in vitro* methodology, it is important to emphasise the importance of such assays in biomaterial testing. However, the current inadequacies of these tests call for further development of reliable *in vitro* characterisation techniques that might predict the success or failure *in vivo* [2].

Here, we modified a coating previously developed by our group [15] by adding calcium (0.5 % and 5 %), the element whose effects we have previously studied [6,11,12] using the *in vitro* and *in vivo* models. The results of such studies, using different techniques (including proteomics), should further characterise the behaviour of the biomaterials and help assess the correlations between the data from *in vitro* and *in vivo* experiments. We found that coagulation and inflammation were the principal biological processes affected by calcium-doping.

The known benefits of Ca have made this element the focus of many investigations; it has been widely employed in developing new biomaterials [28,29]. Moreover, it is used, in the $CaCl_2$ form, as an adjuvant in various medical treatments [30,31].

The Ca-doped coatings developed here adhered well to the metallic substrate without cracking or large porosities.

The analysis of Ca release showed that the formulation with a higher concentration of Ca released a greater amount of Ca^{2+} into the medium

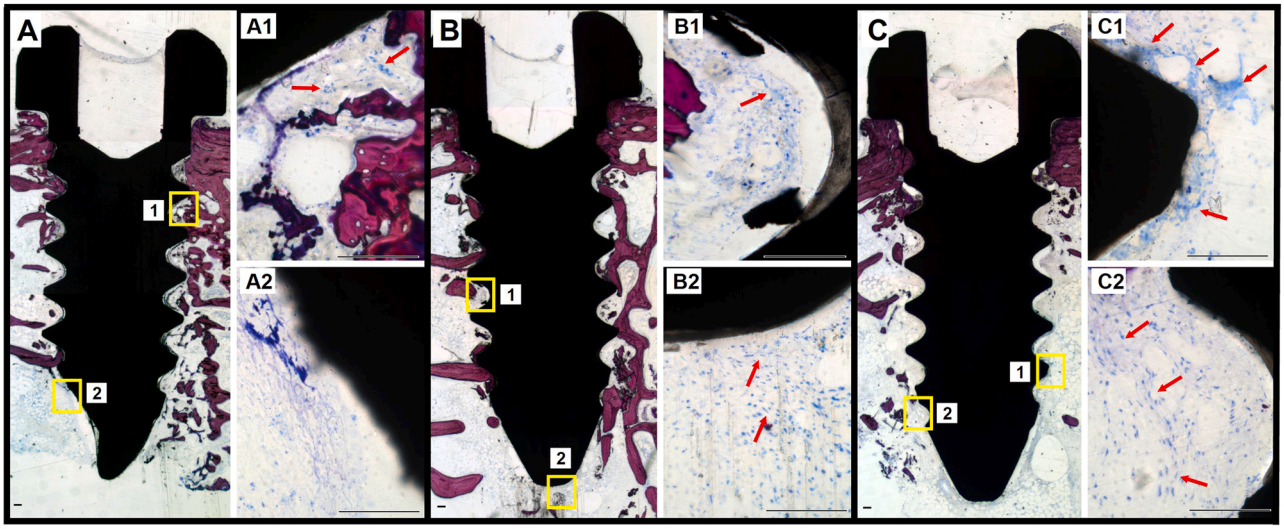

Fig. 7. Microphotographs of control and Ca-doped implant samples processed 5 days after surgery. Panoramic image of MT, MT0.5Ca and MT5Ca samples (A–C). The insets show a higher magnification image of the regions delineated in the corresponding panoramic view. Many large erythrocyte clumps were observed in the MT5Ca sample (C1; red arrows), while fewer and smaller clumps were seen in the MT and MT0.5Ca samples (A1 and B1, respectively; red arrows). Cells of fibroblastic morphology close to the apical implant surface were more abundant in the MT0.5Ca and MT5Ca samples (B2 and C2, respectively; red arrows) than in the MT sample (A2). These fibroblasts tended to be arranged in parallel to the implant surface. Scale bars, 100 μm.

than its low Ca-content counterpart (3.43 mg for MT5Ca *vs* 0.17 mg for MT0.5Ca). The release profiles for the two doped coatings were similar, with a very fast initial release of the ions in the first hours, stabilising throughout the rest of the test. Thus, the Ca^{2+} ions can strongly impact the initial post-implantation period, when coagulation takes place in the wound produced during surgery. Later, in the subsequent stages of tissue regeneration, the effect of these ions would continue at a much lower level.

The effect of Ca-doped coatings on the inflammatory response is reflected by changes in the expression of different inflammation markers expressed by macrophages exposed to these materials *in vitro*. We observed increased expression of IL-1b in the cultures with MT5Ca. The expression of TNF-α rose with increasing calcium content, indicating a possible boost in M1 phenotype activation and, therefore, strengthening the immune response [32,33].

The nLC-MS/MS characterisation of the protein layer adsorbed *in vitro* on the different Ca-enriched coatings revealed many proteins related to the processes associated with the inflammatory response. Among them, a group of proteins belonging to the complement system [34] stands out. Some of these proteins, such as CO5, are involved in activating this cascade [35]. CO5 initiates the spontaneous assembly of the late complement components, C5–C9, into the membrane attack complex [36]. The proteins initiating the cascade of the complement system are found at increased levels on the surfaces enriched in Ca. As the classical pathway of complement activation is dependent on Ca in its early stages, it was not unexpected that the Ca-doped coatings would activate this cascade [37]. The CD5L protein, an inhibitor of apoptosis in macrophages [38], increases its adsorption to surfaces with high calcium content and might augment the inflammatory response. Similarly, the addition of Ca enhanced adsorption of immunoglobulins such as IGHM and KV302, related to the processes of the acute inflammatory response of the immune system [1]. Moreover, increased adsorption of proteins regulating the complement system activation was observed; the CLUS, C4BPA, VTNC and CFAH proteins inhibit and regulate this cascade in its different phases [39].

Two differentially adsorbed apolipoproteins (APOC4 and APOC3) were also detected; these proteins can prevent the activation of the innate immune response and play an anti-inflammatory role [40]. This observation is worth highlighting since the immunomodulatory role of apolipoproteins could be associated with the polarisation of macrophages towards their anti-inflammatory phenotype [41,42].

In this study, the *in vivo* proteomic techniques were used for the first time to analyse the response of a biological system to Ca-doped materials and correlate the results with the *in vitro* protein adsorption data for these materials.

Several proteins found in the *in vivo* proteomic study, CARD6, CD14, SERPING1 and DDOST, confirmed the inflammatory character of the Ca-doped coatings.

CARD6 is involved in complement activation *via* the classical pathway (by activating the NF-κB pathway [43]). Want et al. have verified that targeting CARD6 attenuates spinal cord injury in mice through inhibiting apoptosis, inflammation and oxidative stress [44]. Similarly, the DDOST protein promotes T cell activation associated with inflammatory effects [45].

Some proteins stand out because of their regulatory roles in the complement system. CD14, related to the innate immune responses, acts *via* MyD88, TIRAP and TRAF6, leading to NF-κB activation, cytokine secretion and the inflammatory response [46]. Martin et al. claim that targeting CD14 provides an opportunity to inhibit multiple inflammatory responses [47]. Similarly, the SERPING1 protein is involved in the negative regulation of complement activation by the lectin pathway [48].

The *in vivo* results showed more mesenchymal cells with fibroblastic morphology in the apical portion of the calcium-doped implants than in the non-doped implants. This observation suggests that the proteins related to the immune response, adsorbed on Ca-doped coatings, trigger the inflammatory cascade, leading to the formation of the immune structures [49] (at least during the initial post-implantation period). This behaviour may be normal after such a short time (5 days) and does not imply osseointegration problems at the end of the process; if the reaction is regulated, the fibrous tissue will be reabsorbed. It has been reported that the silicone coatings give rise to a stronger initial inflammatory reaction than Ti materials, which does not diminish their final regenerative potential *in vivo* [50].

Proteins associated with coagulation, key for bone regeneration [51], were also more abundant on the Ca-doped sol-gel surfaces than on un-doped coating in the *in vitro* proteomic study. Ca participates in the formation of the platelet plug, that is, in platelet aggregation and in the polymerisation of fibrin that gives rise to coagulation [52]. In the presence of Ca ions released from the coating, the platelet activation

and, therefore, coagulation are to be expected. THRB, also known as coagulation factor II, belongs to the common pathway of the coagulation cascade. It can trigger blood coagulation through its conversion to the protease thrombin, activating platelet formation [53]. Platelet factor 4 (PLF4) is a small cytokine released from alpha-granules of activated platelets during platelet aggregation. It promotes blood coagulation by moderating the effects of heparin-like molecules and is involved in wound repair and inflammation [54]. The PLMN protein plays an important role in activating the plasminogen system, the key step in the fibrinolysis process. The coagulation system is one of the main initiators of blood clotting after a trauma. After this stage, the plasminogen system acts during the degradation of the extracellular matrix and the consequent tissue remodelling and angiogenesis, which leads to correct tissue healing [55]. The FIBA protein is associated with different biological functions, such as blood clotting and fibrinolysis [56]. The PROS protein participates in the regulation of the blood coagulation pathway [57]. This plasma protein helps prevent coagulation and stimulates fibrinolysis. The VTNC, in addition to its role as an inhibitor of complement cascade activation, could interact with the coagulation cascade, contributing to thrombus formation, wound repair, vascular homeostasis, and tissue regeneration [58]. The HRG protein is also involved in these stages of regeneration [59]. It could function as an antifibrinolytic and anticoagulant modulator and regulate platelet function *in vivo* [60]. In PANTHER analysis, coagulation was the most important function, and the only one common to all coatings supplemented with Ca.

This behaviour was confirmed by the *in vivo* proteomic study. FBLN1, G1U978 and SERPING1 proteins, involved in blood coagulation, also showed preferential binding to the Ca-doped material surfaces. FBLN1 may be involved in haemostasis and thrombosis as it can bind fibrinogen and incorporate itself into clots [61]. SERPING1 is a plasma protease involved in the intrinsic coagulation and fibrinolytic pathways. In the coagulation cascade, this protease inactivates plasma kallikrein, factor XIIa and factor XIIf [62].

The histological study showed that the implant threads contained the remnants of the fibrin-rich matrix from the blood clot formed after surgery. The number and size of the erythrocyte clusters were greater around the MT5Ca coating than those observed for MT and MT0.5Ca. This suggests that the addition of Ca results in increased coagulation.

The *in vitro* proteomic study demonstrated enhanced adsorption of three proteins related to bone regeneration, VTNC, PEDF and TETN, on the 0.5 % Ca-doped coatings. The VTNC could also favour osteoblastic differentiation [63]. The surfaces that adsorb more VTNC increase the adhesion and proliferation of osteoblasts and, therefore, improve osteoconduction [64]. The study of Feng et al. has shown that PEDF improves osteoblastic differentiation and increases mineralisation of the bone matrix [65]. Other reports, such as studies by Venturi et al., have confirmed that the lack of PEDF leads to bone defects and frequent fractures [66]. Gattu et al. [67] and Li et al. [68] have reported that PEDF improves osteoblastic differentiation of human and mouse mesenchymal stem cells and increases osteoblastic mineralisation *in vitro*. The TETN protein has been linked to the correct development of bone tissue. This protein is involved in new tissue formation and matrix remodelling in the cutaneous wound healing processes [69], similar to the healing processes of bone fractures [70]. Furthermore, using an *in vitro* bovine mineralizing system, Wewer et al. examined osteoblastic cells at different times during their growth and differentiation. This *in vitro* study has shown that TETN is expressed during bone formation [71].

Among the proteins differentially expressed in the tissues surrounding the different implants *in vivo*, FBN1 and AHSG were found in increased amounts close to the Ca-doped coatings and the MYOC protein in the tissue in contact with the MT. The FBN1 protein is linked to negative regulation of osteoclast development [72]. The highest expression of this protein was observed close to the MT0.5Ca implants; it can lead to inhibition of osteoclastogenesis, which would favour the process of bone regeneration. The AHSG, whose expression increased in the vicinity of MT5Ca, is related to the negative regulation of bone mineralisation [73]. MYOC is involved in bone formation and promotes osteoblast differentiation in a dose-dependent manner through mitogen-activated protein kinase signalling [74]. The abundance of this protein was reduced in the tissue near the Ca-doped coatings; it decreased drastically for the MT5Ca implants.

Thus, we can conclude that there is a correlation between *in vitro* and *in vivo* proteomic results. Moreover, there is an optimal formulation for bone regeneration, *i.e.*, MT0.5Ca. For coatings with 5 % Ca, the regeneration was diminished, and a negative effect was observed using different proteomic techniques. A more detailed histological study with longer-lasting experiments will be needed to confirm these trends.

In the light of the results presented here, we can conclude that adding Ca to the biomaterials causes an increase in the initial inflammation and strengthens coagulation. Furthermore, the proteomic results correlate with histological observations made after *in vivo* experiment.

Although further research is needed in this area, it is clear that proteomics offers a powerful toolset for predicting *in vivo* responses and characterising biomaterials. It allowed us to evaluate the regenerative potential of new Ca-doped sol-gel surfaces in short experiments. At the same time, we obtained valuable data on several processes important in the healing of bone tissue.

5. Conclusion

The new Ca-doped sol-gel materials, capable of releasing Ca^{2+} ions, were characterised by performing *in vitro* and *in vivo* tests, which supplied valuable data after an *in vivo* proteomic analysis. The Ca-doping affected the *in vitro* responses of human osteoblasts and TPH-1 monocytes, and protein adsorption onto the coatings. The changes in TNF-α, IL-1b, TGF-β and IL-10 levels showed that the inflammatory responses depend on the amount of Ca incorporated into the materials. Moreover, the *in vitro* and *in vivo* proteomics revealed increased adhesion of a cluster of proteins related to the immune, coagulation and regenerative processes. Adding calcium to the coatings increased the adsorption of proteins involved in the immune response, such as VTNC, CO5, C4BPA and KV302 *in vitro*, and the levels of CARD6, DDOST and CD14 *in vivo*. It similarly affected the coagulation activity, for instance, the abundance of FIBA, THRB or PLMN *in vitro* and FBLN1and G1U978 *in vivo*. Moreover, changes in the levels of proteins such as TETN or PEDF (*in vitro*) and FBN1, AHSG or MYOC (*in vivo*) indicate that MT0.5Ca formulation is the most likely to have good osteogenic properties. The proteomic results were consistent with the biological responses observed using the histological examination. The proteomic analysis showed a good correlation between the *in vitro* and *in vivo* tests (for short experimental periods). Consequently, we can conclude that these methods can be useful in developing new biomaterials.

CRediT authorship contribution statement

I. García-Arnáez: Formal analysis, Investigation, Writing – original draft, Writing – review & editing. **F. Romero-Gavilán:** Investigation, Writing – review & editing. **A. Cerqueira:** Methodology, Investigation. **F. Elortza:** Data curation, Writing – review & editing. **M. Azkargorta:** Investigation, Data curation. **F. Muñoz:** Investigation, Data curation. **M. Mata:** Investigation, Data curation. **J.J. Martín de Llano:** Investigation, Data curation, Writing – review & editing. **J. Suay:** Conceptualization, Writing – review & editing, Funding acquisition. **M. Gurruchaga:** Conceptualization, Writing – review & editing, Funding acquisition. **I. Gon Goñi:** Conceptualization, Writing – review & editing, Funding acquisition.

Declaration of Competing Interest

The authors declare that they have no known competing financial interests or personal relationships that could have appeared to influence

the work reported in this paper.

Data Availability

Data will be made available on request.

Acknowledgements

This work was supported by Ministerio de Ciencia e Innovación (PID2020-113092RB-C21), University of the Basque Country UPV/EHU (MARSA21/07), Basque Government (PRE_2016_1_0141), Universitat Jaume I (UJI-B2021-25) and Generalitat Valenciana (APOSTD/2020/036, PROMETEO/2020/069). The authors would like to thank for technical and staff support provided by SGIker (UPV/EHU/ ERDF, EU), and the company GMI Dental Implantology SL for producing the titanium discs.

Appendix A. Supporting information

Supplementary data associated with this article can be found in the online version at doi:10.1016/j.colsurfb.2022.112962.

References

[1] F. Romero-Gavilan, A.M. Sánchez-Pérez, N. Araújo-Gomes, M. Azkargorta, I. Iloro, F. Elortza, et al., Proteomic analysis of silica hybrid sol-gel coatings: a potential tool for predicting the biocompatibility of implants in vivo, Biofouling 33 (2017) 676–689, https://doi.org/10.1080/08927014.2017.1356289.
[2] G. Hulsart-Billström, J.I. Dawson, S. Hofmann, R. Müller, M.J. Stoddart, M. Alini, et al., A surprisingly poor correlation between in vitro and in vivo testing of biomaterials for bone regeneration: results of a multicentre analysis, Eur. Cells Mater. 31 (2016) 312–322, https://doi.org/10.22203/eCM.v031a20.
[3] J. Bailey, M. Thew, M. Balls, An analysis of the use of animal models in predicting human toxicology and drug safety, Alter. Lab. Anim. 42 (2014) 181–199, https://doi.org/10.1177/026119291404200306.
[4] L.T. Allen, M. Tosetto, I.S. Miller, D.P. O'Connor, S.C. Penney, I. Lynch, et al., Surface-induced changes in protein adsorption and implications for cellular phenotypic responses to surface interaction, Biomaterials 27 (2006) 3096–3108, https://doi.org/10.1016/j.biomaterials.2006.01.019.
[5] Z. Othman, B. Cillero Pastor, S. van Rijt, P. Habibovic, Understanding interactions between biomaterials and biological systems using proteomics, Biomaterials 167 (2018) 191–204, https://doi.org/10.1016/j.biomaterials.2018.03.020.
[6] F. Romero-Gavilán, N. Araújo-Gomes, A. Cerqueira, I. García-Arnáez, C. Martínez-Ramos, M. Azkargorta, et al., Proteomic analysis of calcium-enriched sol–gel biomaterials, J. Biol. Inorg. Chem. 24 (2019) 563–574, https://doi.org/10.1007/s00775-019-01662-5.
[7] A. Hoppe, N.S. Güldal, A.R. Boccaccini, A review of the biological response to ionic dissolution products from bioactive glasses and glass-ceramics, Biomaterials 32 (2011) 2757–2774, https://doi.org/10.1016/j.biomaterials.2011.01.004.
[8] E. Anitua, L. Piñas, A. Murias, R. Prado, R. Tejero, Effects of calcium ions on titanium surfaces for bone regeneration, Colloids Surf. B Biointerfaces 130 (2015) 173–181.
[9] J. Lorenzo, M. Horowitz, Y. Choi, Osteoimmunology: interactions of the bone and immune system, Endocr. Rev. 29 (2008) 403–440.
[10] J. Gessmann, D. Seybold, E. Peter, T.A. Schildhauer, M. Köller, Plasma clots gelled by different amounts of calcium for stem cell delivery, Langenbeck's Arch. Surg. 398 (2013) 161–167, https://doi.org/10.1007/s00423-012-1015-8.
[11] E. Anitua, A. Cerqueira, F. Romero-Gavilán, I. García-Arnáez, C. Martinez-Ramos, S. Ozturan, et al., Influence of calcium ion-modified implant surfaces in protein adsorption and implant integration, Int. J. Implant Dent. 7 (2021) 32, https://doi.org/10.1186/s40729-021-00314-1.
[12] F. Romero-Gavilán, A. Cerqueira, E. Anitua, R. Tejero, I. García-Arnáez, C. Martinez-Ramos, et al., Protein adsorption/desorption dynamics on Ca-enriched titanium surfaces: biological implications, JBIC J. Biol. Inorg. Chem. 26 (2021) 715–726.
[13] Y. Zhong, X. Chen, H. Peng, Z. Ding, Y. Yan, Developing novel Ca-zeolite/poly (amino acid) composites with hemostatic activity for bone substitute applications, J. Biomater. Sci. Polym. Ed. 29 (2018) 1994–2010.
[14] M.M. Markiewski, B. Nilsson, K. Nilsson Ekdahl, T.E. Mollnes, J.D. Lambris, Complement and coagulation: strangers or partners in crime, Trends Immunol. 28 (2007) 184–192, https://doi.org/10.1016/j.it.2007.02.006.
[15] M. Martínez-Ibáñez, M.J. Juan-Díaz, I. Lara-Saez, A. Coso, J. Franco, M. Gurruchaga, et al., Biological characterization of a new silicon based coating developed for dental implants, J. Mater. Sci. Mater. Med. 27 (2016) 80.
[16] N. Araújo-Gomes, F. Romero-Gavilán, I. García-Arnáez, C. Martínez-Ramos, A. M. Sánchez-Pérez, M. Azkargorta, et al., Osseointegration mechanisms: a proteomic approach, J. Biol. Inorg. Chem. 23 (2018) 459–470, https://doi.org/10.1007/s00775-018-1553-9.
[17] A. Cerqueira, F. Romero-Gavilan, N. Araujo-Gomes, I. Garcia-Arnaez, C. Martinez-Ramos, S. Ozturan, et al., A possible use of melatonin in the dental field: protein adsorption and in vitro cell response on coated titanium, Mater. Sci. Eng. C 116 (2020), 111262.
[18] A. Cerqueira, F. Romero-Gavilán, I. García-Arnáez, C. Martinez-Ramos, S. Ozturan, R. Izquierdo, et al., Characterization of magnesium doped sol-gel biomaterial for bone tissue regeneration: The effect of Mg ion in protein adsorption, Mater. Sci. Eng. C 125 (2021), 112114.
[19] J.R. Wiśniewski, A. Zougman, N. Nagaraj, M. Mann, Universal sample preparation method for proteome analysis, Nat. Methods 6 (2009) 359–362, https://doi.org/10.1038/nmeth.1322.
[20] J. Cox, M. Mann, MaxQuant enables high peptide identification rates, individualized ppb-range mass accuracies and proteome-wide protein quantification, Nat. Biotechnol. 26 (2008) 1367–1372.
[21] S. Tyanova, T. Temu, P. Sinitcyn, A. Carlson, M.Y. Hein, T. Geiger, et al., The Perseus computational platform for comprehensive analysis of (prote) omics data, Nat. Methods 13 (2016) 731–740.
[22] T.U. Consortium, UniProt: the universal protein knowledgebase in 2021, Nucleic Acids Res. 49 (2021) D480–D489.
[23] K. Donath, G. Breuner, A method for the study of undecalcified bones and teeth with attached soft tissues* The Säge-Schliff (sawing and grinding) Technique, J. Oral Pathol. Med 11 (1982) 318–326.
[24] J. Lackó, L. Géza, A simple differential staining method for semi-thin sections of ossifying cartilage and bone tissues embedded in epoxy resin, Mikroskopie 31 (1975) 1–4.
[25] M.C. Carroll, The complement system in B cell regulation, Mol. Immunol. 41 (2004) 141–146.
[26] S. Tripathi, Å. Flobak, K. Chawla, A. Baudot, T. Bruland, L. Thommesen, et al., The gastrin and cholecystokinin receptors mediated signaling network: a scaffold for data analysis and new hypotheses on regulatory mechanisms, BMC Syst. Biol. 9 (2015) 40, https://doi.org/10.1186/s12918-015-0181-z.
[27] R.L. Medcalf, Fibrinolysis, inflammation, and regulation of the plasminogen activating system, J. Thromb. Haemost. 5 (2007) 132–142.
[28] A. Diez-Escudero, M. Espanol, M.-P. Ginebra, Synthetic bone graft substitutes: calcium-based biomaterials, Dent. Implant. Bone Grafts (2020) 125–157.
[29] L.-J. Yi, J.-F. Li, M.-G. Ma, Y.-J. Zhu, Nanostructured calcium-based biomaterials and their application in drug delivery, Curr. Med Chem. 27 (2020) 5189–5212.
[30] G.B. Patel, H. Zhou, A. Ponce, W. Chen, Mucosal and systemic immune responses by intranasal immunization using archaeal lipid-adjuvanted vaccines, Vaccine 25 (2007) 8622–8636.
[31] S. Gould-Fogerite, M.T. Kheiri, F. Zhang, Z. Wang, A.J. Scolpino, E. Feketeova, et al., Targeting immune response induction with cochleate and liposome-based vaccines, Adv. Drug Deliv. Rev. 32 (1998) 273–287.
[32] A. Sica, P. Larghi, A. Mancino, L. Rubino, C. Porta, M.G. Totaro, et al., Macrophage polarization in tumour progression, Semin. Cancer Biol 18 (2008) 349–355.
[33] W. Xuan, Q. Qu, B. Zheng, S. Xiong, G. Fan, The chemotaxis of M1 and M2 macrophages is regulated by different chemokines, J. Leukoc. Biol. 97 (2015) 61–69.
[34] C.J. Janeway, P. Travers, M. Walport, The Complement System and Innate Immunity. Immunobiol. Immune Syst. Heal. Dis. 5th editio, Garland Science, New York, 2001, pp. 61–81.
[35] D. Ricklin, G. Hajishengallis, K. Yang, J.D. Lambris, Complement: a key system for immune surveillance and homeostasis, Nat. Immunol. 11 (2010) 785–797, https://doi.org/10.1038/ni.1923.
[36] J.-A. Haefliger, J. Tschopp, N. Vial, D.E. Jenne, Complete primary structure and functional characterization of the sixth component of the human complement system: identification of the C5b-binding domain in complement C6, J. Biol. Chem. 264 (1989) 18041–18051.
[37] M.V. Carroll, R.B. Sim, Complement in health and disease, Adv. Drug Deliv. Rev. 63 (2011) 965–975.
[38] T. Nishikido, J. Oyama, A. Shiraki, H. Komoda, K. Node, Deletion of apoptosis inhibitor of macrophage (AIM)/CD5L attenuates the inflammatory response and infarct size in acute myocardial infarction, J. Am. Heart Assoc. 5 (2016), e002863.
[39] N.S. Merle, S.E. Church, V. Fremeaux-Bacchi, L.T. Roumenina, Complement system part I–molecular mechanisms of activation and regulation, Front. Immunol. 6 (2015) 262.
[40] N. Cho, S. Seong, Apolipoproteins inhibit the innate immunity activated by necrotic cells or bacterial endotoxin, Immunology 128 (2009) e479–e486.
[41] Q. Li, Z. Zhai, W. Ma, Z. Qian, Anti-inflammatory effects of apoprotein AI are mediated via modulating macrophage polarity, Zhonghua Xin Xue Guan Bing. Za Zhi 42 (2014) 132–135.
[42] D. Baitsch, H.H. Bock, T. Engel, R. Telgmann, C. Müller-Tidow, G. Varga, et al., Apolipoprotein E induces antiinflammatory phenotype in macrophages, Arterioscler. Thromb. Vasc. Biol. 31 (2011) 1160–1168.
[43] S.S. Kim, C.H. Ahn, M.R. Kang, Y.R. Kim, H.S. Kim, N.J. Yoo, et al., Expression of CARD6, an NF-κB activator, in gastric, colorectal and oesophageal cancers, Pathology 42 (2010) 50–53.
[44] J.L. Wang, X. Luo, L. Liu, Targeting CARD6 attenuates spinal cord injury (SCI) in mice through inhibiting apoptosis, inflammation and oxidative stress associated ROS production, Aging 11 (2019) 12213.
[45] J.E. Smith-Garvin, G.A. Koretzky, M.S. Jordan, T cell activation, Annu. Rev. Immunol. 27 (2009) 591–619.
[46] J.D. Lee, K. Kato, P.S. Tobias, T.N. Kirkland, R.J. Ulevitch, Transfection of CD14 into 70Z/3 cells dramatically enhances the sensitivity to complexes of lipopolysaccharide (LPS) and LPS binding protein, J. Exp. Med. 175 (1992) 1697–1705.

[47] T.R. Martin, M.M. Wurfel, I. Zanoni, R. Ulevitch, Targeting innate immunity by blocking CD14: Novel approach to control inflammation and organ dysfunction in COVID-19 illness, EBioMedicine (2020) 57.
[48] K.S. Aulak, A.E. Davis III, V.H. Donaldson, R.A. Harrison, Chymotrypsin inhibitory activity of normal C1–inhibitor and a P1 Arg to His mutant: evidence for the presence of overlapping reactive centers, Protein Sci. 2 (1993) 727–732.
[49] N. Araújo-Gomes, F. Romero-Gavilán, A.M. Sánchez-Pérez, M. Gurruchaga, M. Azkargorta, F. Elortza, et al., Characterization of serum proteins attached to distinct sol–gel hybrid surfaces, J. Biomed. Mater. Res. Part B Appl. Biomater. 106 (2018) 1477–1485.
[50] F. Romero-Gavilan, N. Araújo-Gomes, A.M. Sánchez-Pérez, I. García-Arnáez, F. Elortza, M. Azkargorta, et al., Bioactive potential of silica coatings and its effect on the adhesion of proteins to titanium implants, Colloids Surf. B Biointerfaces (2018) 162, https://doi.org/10.1016/j.colsurfb.2017.11.072.
[51] F. Loi, L.A. Córdova, J. Pajarinen, T. Lin, Z. Yao, S.B. Goodman, Inflammation, fracture and bone repair, Bone 86 (2016) 119–130.
[52] A.D. Leavitt, What for platelet factor 4, Blood 110 (2007) 1090, https://doi.org/10.1182/blood-2007-05-091363.
[53] N. Pozzi, E. Di Cera, Prothrombin structure: unanticipated features and opportunities, 2014.
[54] R. Eisman, S. Surrey, B. Ramachandran, E. Schwartz, M. Poncz, Structural and functional comparison of the genes for human platelet factor 4 and PF4alt, 1990.
[55] C. Wehner, K. Janjić, H. Agis, Relevance of the plasminogen system in physiology, pathology, and regeneration of oral tissues–from the perspective of dental specialties, Arch. Oral. Biol. 74 (2017) 136–145.
[56] M.W. MOSESSON, Fibrinogen and fibrin structure and functions, J. Thromb. Haemost. 3 (2005) 1894–1904.
[57] A.J. Chu, Blood coagulation as an intrinsic pathway for proinflammation: A mini review, Inflamm. Allergy - Drug Targets 9 (2010) 32–44, https://doi.org/10.2174/187152810791292890.
[58] R.M. Salasznyk, W.A. Williams, A. Boskey, A. Batorsky, G.E. Plopper, Adhesion to vitronectin and collagen I promotes osteogenic differentiation of human mesenchymal stem cells, J. Biomed. Biotechnol. (2004) 2004.
[59] A.T. Long, E. Kenne, R. Jung, T.A. Fuchs, T. Renné, Contact system revisited: an interface between inflammation, coagulation, and innate immunity, J. Thromb. Haemost. 14 (2016) 427–437.
[60] S. Wakabayashi, T. Koide, Histidine-rich glycoprotein: a possible modulator of coagulation and fibrinolysis, Semin. Thromb. Hemost. 37 (2011) 389–394.
[61] H. Tran, A. Tanaka, S.V. Litvinovich, L.V. Medved, C.C. Haudenschild, W. S. Argraves, The Interaction of Fibulin-1 with Fibrinogen: A POTENTIAL ROLE IN HEMOSTASIS AND THROMBOSIS (*), J. Biol. Chem. 270 (1995) 19458–19464.
[62] D. Holcomb, A. Alexaki, N. Hernandez, R. Hunt, K. Laurie, J. Kames, et al., Gene variants of coagulation related proteins that interact with SARS-CoV-2, PLoS Comput. Biol. 17 (2021), e1008805.
[63] D.I. Leavesley, A.S. Kashyap, T. Croll, M. Sivaramakrishnan, A. Shokoohmand, B. G. Hollier, et al., Vitronectin—Master controller or micromanager? IUBMB Life 65 (2013) 807–818.
[64] D.M. Rivera-Chacon, M. Alvarado-Velez, C.Y. Acevedo-Morantes, S.P. Singh, E. Gultepe, D. Nagesha, et al., Fibronectin and vitronectin promote human fetal osteoblast cell attachment and proliferation on nanoporous titanium surfaces, J. Biomed. Nanotechnol. 9 (2013) 1092–1097.
[65] F. Li, N. Song, J. Tombran-Tink, C. Niyibizi, Pigment epithelium derived factor suppresses expression of Sost/Sclerostin by osteocytes: implication for its role in bone matrix mineralization, J. Cell Physiol. 230 (2015) 1243.
[66] G. Venturi, A. Gandini, E. Monti, L.D. Carbonare, M. Corradi, M. Vincenzi, et al., Lack of expression of SERPINF1, the gene coding for pigment epithelium-derived factor, causes progressively deforming osteogenesis imperfecta with normal type I collagen, J. Bone Min. Res. 27 (2012) 723–728.
[67] A.K. Gattu, E.S. Swenson, Y. Iwakiri, V.T. Samuel, N. Troiano, R. Berry, et al., Determination of mesenchymal stem cell fate by pigment epithelium-derived factor (PEDF) results in increased adiposity and reduced bone mineral content, FASEB J. 27 (2013) 4384–4394.
[68] F. Li, N. Song, J. Tombran-Tink, C. Niyibizi, Pigment epithelium-derived factor enhances differentiation and mineral deposition of human mesenchymal stem cells, Stem Cells 31 (2013) 2714–2723.
[69] P. Martin, J. Hopkinson-Woolley, J. McCluskey, Growth factors and cutaneous wound repair, Prog. Growth Factor Res. 4 (1992) 25–44.
[70] T.A. Einhorn, The cell and molecular biology of fracture healing, Clin. Orthop. Relat. Res 355 (1998) S7–S21.
[71] U.M. Wewer, K. Ibaraki, P. Schjørring, M.E. Durkin, M.F. Young, R. Albrechtsen, A potential role for tetranectin in mineralization during osteogenesis, J. Cell Biol. 127 (1994) 1767–1775.
[72] K. Tiedemann, I. Boraschi-Diaz, I. Rajakumar, J. Kaur, P. Roughley, D.P. Reinhardt, et al., Fibrillin-1 directly regulates osteoclast formation and function by a dual mechanism, J. Cell Sci. 126 (2013) 4187–4194.
[73] Y.-J. Yang, Y.-B. Wang, S.-F. Lei, J.-R. Long, H. Shen, L.-J. Zhao, et al., AHSG gene polymorphisms are associated with bone mineral density in Caucasian nuclear families, Eur. J. Epidemiol. 22 (2007) 527–532.
[74] H.S. Kwon, T.V. Johnson, S.I. Tomarev, Myocilin stimulates osteogenic differentiation of mesenchymal stem cells through mitogen-activated protein kinase signaling, J. Biol. Chem. 288 (2013) 16882–16894.